Strong and Weak Electric Field Interfering: Capacitive Icing Detection and Capacitive Energy Harvesting on a 220-kV High-Voltage Overhead Power Line

Michael J. Moser, *Student Member, IEEE*, Thomas Bretterklieber, *Member, IEEE*, Hubert Zangl, *Member, IEEE*, and Georg Brasseur, *Fellow, IEEE*

***Abstract*—This paper focuses on problems which arise when both a power-harvesting system based on a capacitive principle and a capacitive measurement device [i.e., a capacitance-to-digital converter (CDC)] are used in one electronic system to build up an autonomous measurement device for icing detection on a high-voltage overhead power line. The overall capacitance of the measurement circuitry between the conductor and the energy harvester shell must remain within a well-defined range to keep the energy-harvesting circuitry operational and to operate the CDC within its specifications. A decoupling solution for both the data path and the power supply unit has been implemented and verified experimentally in a high-voltage laboratory and a field test.**

***Index Terms*—Capacitance measurement, decoupling of systems, energy harvesting, galvanic isolator, high-voltage overhead power line, icing detection, online condition monitoring, optical coupler, power system reliability, wireless communication.**

I. Introduction

THE distribution of electric energy by means of high-voltage overhead power lines is a very common technique as installation costs are low, maintenance costs are reasonable, and operation times are long (often several decades). However, overhead power lines are subject to environmental conditions and changes. In order to maintain a safe operation, regular inspections of the power lines are needed. This condition monitoring is usually done by means of on-ground and helicopter-aided visual inspection. Monitoring and diagnostic systems (compare [1] and [2]) are usually wired and thus limited, e.g., to transformer stations. As wired monitoring systems require expensive communication, particularly over long distances, they are not widely implemented today [3]. Certain weather conditions—although they occur rather rarely—pose potential problems to the power line. For instance, in 1998, 150 transmission towers collapsed in a Canadian power system due to ice accumulation [4]. The measurement of conductor icing in an early stage is thus of interest for power supply companies operating lines in endangered areas [5].

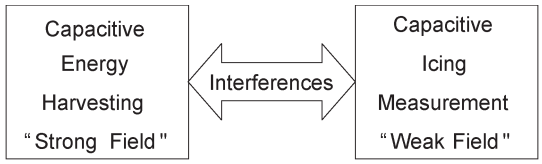

Fig. 1. Two systems need to be integrated: A capacitive energy-harvesting system with an electric field strength in megavolts per meter in the vicinity of the conductor and a capacitive icing measurement system with an electric field strength on the order of magnitude of volts per meter.

The main aim of this paper is to discuss problems that occur when a capacitive icing measurement unit and a capacitive power-harvesting unit are integrated in a measurement system as illustrated in Fig. 1. Aside from weather conditions, the system is exposed to high currents exceeding 1000 A and line voltages of 220 kV in close vicinity. Details on associated problems and the developed solution are given in Section II. In Section III, the experimental evaluation of the proposed solution is presented. This solution has been implemented and tested at the high-voltage laboratory of the Graz University of Technology and is currently in a field test on a 220-kV overhead power line.

II. Combining Capacitive Icing Detection and Capacitive Energy Harvesting

Ice forming and its accumulation on the surface of high-voltage power transmission lines can lead to an increased line sag, i.e., the distance between the line and the ground decreases. Eventually, lines have to be taken offline to deice them either by special circuitry or even manually. Therefore, icing should be detected as early as possible to trigger countermeasures [5]. Existing systems (compare, e.g., [6]–[8]) mainly rely on weather data collection to calculate and predict icing conditions. Other systems measure, e.g., the weight of one bundle of conductors or detect freezing rain conditions [4]. However, these principles are indirect and may always be afflicted with

Manuscript received April 6, 2010; revised August 11, 2010; accepted November 4, 2010. Date of publication December 10, 2010; date of current version June 15, 2011.

The authors are with the Institute of Electrical Measurement and Measurement Signal Processing, Graz University of Technology, 8010 Graz, Austria (e-mail: michael.moser@tugraz.at; thomas.bretterklieber@tugraz.at; hubert.zangl@tugraz.at; georg.brasseur@tugraz.at).

Color versions of one or more of the figures in this paper are available online at http://ieeexplore.ieee.org.

Digital Object Identifier 10.1109/TIE.2010.2098362

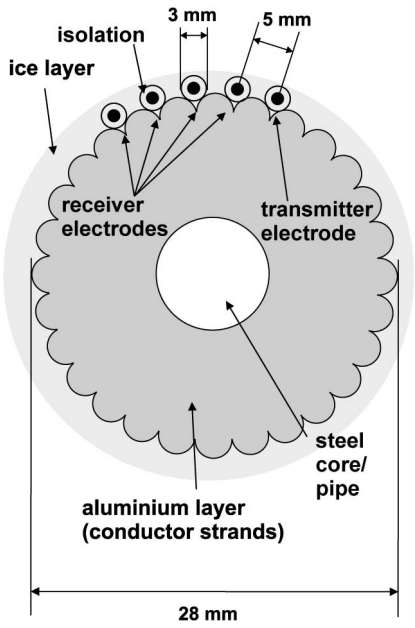

Fig. 2. Measurement capacitances between a common transmitter electrode and multiple receiver electrodes are evaluated. The sensor electrodes consist of electrically isolated wires PTFE (Teflon) that follow the twisting of the conductor strands. The sensor characteristics are determined by the electrode distance, the thickness of the isolation layer, and the electrode length.

a certain level of uncertainty as they do not measure the actual occurrence of the ice layer. In contrast to this, the main advantage of capacitive icing measurement [9] is the direct measurement. In comparison to other methods (optical measurement, microwaves, and ultrasound), it even allows for detecting thin layers, i.e., detecting the icing process at the early stages of accumulation.

A. Icing Detection by Means of Capacitive Sensing

Capacitive sensing technology is frequently used for humidity measurement [10]. For icing detection, not only the presence but also the layer thickness is of interest. In order to achieve this, four measurement capacitors defined by a single transmitter (HF excitation) and multiple multiplexed receivers are continuously evaluated (compare Fig. 2). The measurement capacitances differ in interelectrode distance, thus having different nominal capacitances. As the intercapacitance distances are different for each measurement capacitance, the changes in capacitance due to layers of ice or water covering the electrodes are similar yet unique for any electrode distance.

Fig. 3 shows an illustration of the measurement principle. With capacitive sensing, the coupling between a common transmitter electrode T and two receiver electrodes R_1 and R_2 is determined. When the permittivity is low (air, $\varepsilon_r = 1$), the displacement current is low and concentrated around the transmitter. Thus, only a low coupling can be observed. When an ice layer $(\varepsilon_r > 2)$ forms on the surface, then the displacement current increases due to the higher permittivity. Thus, the coupling capacitance increases. However, when the layer becomes thicker and thicker, the displacement current is directed further away. This leads to a decreasing coupling with respect to receiver R_1. Eventually, also the coupling to receiver

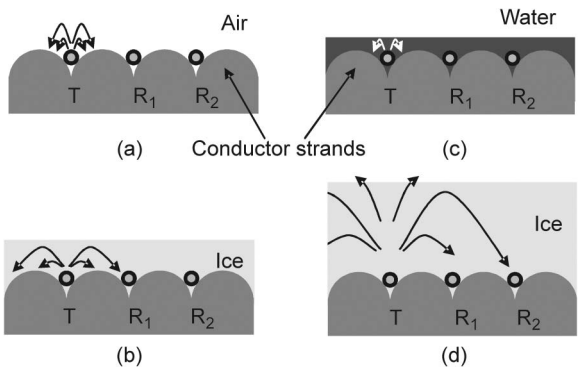

Fig. 3. Illustration of the measurement principle. Compared to (a) air, the displacement current is increased for ice-covered electrodes due to the higher permittivity of (b) ice. Thus, also the coupling between transmitter T and receivers R_1 and R_2 increases. (d) For increasing the thickness of the ice layer, the displacement current is more and more directed away from the electrodes, and the coupling capacitance starts to decrease again. (c) For very high permittivities, the displacement current is directed toward the conductor, even for thin layers. Consequently, water leads to reduced coupling capacitances, and ice leads to increased coupling capacitances.

R_2 decreases, but this occurs for thicker ice layers than for receiver R_1. When the permittivity of a thin layer becomes very high (water, $\varepsilon_r = 80$), then the displacement current is strongly increased. However, due to the strong coupling to the conductor, the field remains concentrated around the transmitter, and the coupling to the receivers is low. Consequently, the principle permits the determination of ice thickness due to the plurality of electrodes. Furthermore, ice can be distinguished from water due to the different impact on the coupling.

The parasitic coupling between the sensor electrodes and the ground (i.e., the conductor) is eliminated by a low impedance measurement principle: As long as the input impedance of the measurement circuitry is significantly lower than the impedance of the parasitic capacitance, almost the entire current will flow into the measurement circuitry. This current is proportional to the coupling capacitance. A more detailed description of low impedance measurement circuitry is given, e.g., in [18].

A typical signal trace can be seen in Fig. 4. The measurement is carried out by means of capacitance-to-digital converters (CDCs), which evaluate up to 16 measurement electrodes in the picofarad range with a resolution of 16 bit or better. As can be seen in Fig. 4, for very small ice layers (below a 0.5-mm thickness in the current setup), the measured capacitance is decreasing to a minimum. This is due to a better coupling between the measurement electrodes and the "measurement ground" (conductor). The effect is commonly referred to as "shielding mode" [11]. With increasing layer thickness, this effect is compensated. Furthermore, the resulting capacitance exceeds the "dry" value, reaches a maximum, and—depending on the electrode distance—decreases again. For a wet conductor, the "shielding" effect (i.e., a decreasing measured capacitance) dominates as the permittivity of water $(\varepsilon_r \approx 80)$ is much higher than the permittivity of ice ($\varepsilon_r \approx 3$–5), and a thick layer of water (exceeding several millimeters) may not occur as liquid water will drop off instantly. As the curve shape is similar but unique for any electrode distance, multiple measurement capacitances can be evaluated to obtain an unambiguous result for the ice layer thickness and quality.

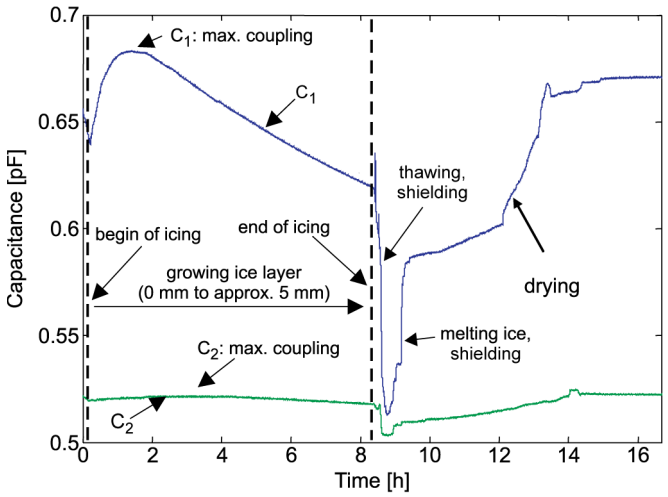

Fig. 4. Measurement signals from an air humidity icing experiment for two different electrode distances. The measurement traces C_1 and C_2 are obtained for the near electrode R_1 and the far electrode R_2, respectively [9]. For a small interelectrode distance (R_1), the nominal capacitance and also the absolute capacitance change due to ice and water are larger than those for a larger interelectrode distance (R_2). At the beginning of the experiment (0 h), no ice nor water is present on the conductor. During approximately 8 h, ice is forming and constantly gaining in thickness. Then, the cooling system is turned off, and the ice layer starts melting. Water is held in that half-frozen layer for a short while, and after approximately 10 h, a drying process is observed.

In our first icing detection experiments, the measurement electrodes are built up by a coaxial cable with a removed (outer) shielding layer in the sensing area. This allows for easy prototyping and modification during experiments. For the high-voltage environment, a special Teflon-isolated and corona-proof cable that is certified for 5 kV between the conductor and the environment and between the conductor and the shielding layer, respectively, is used. In the current setup, the sensor electrode length is covering approximately half the length of the twist of the stranded conductor, thus covering half of the conductor circumference. The electrode geometry can be easily modified to cover the whole conductor circumference. Increasing interelectrode distances also allows for the detection of thicker ice layers.

B. Capacitive Energy Harvesting

It has been shown that energy can be harvested from the alternating electric field between the conductor line and the surrounding earth by inserting a conductive shell between the conductor and earth, thus forming a capacitive voltage divider [12]. Compared to energy harvesting from the magnetic field (compare [13] and [14]), its main advantage is the independence from the load status. In addition, it is not depending on weather conditions (drawback of solar energy [15]) and does not require maintenance at regular intervals as battery-powered systems do. This energy-harvesting principle allows for an autonomous measurement device which could work for years without maintenance. For the proposed geometry, the displacement current to the environment amounts to several hundreds of microamperes [12]. The field strength far from the conductor is low, and most of the potential decrease occurs in the vicinity of the conductor. Thus, increasing the distance between the harvester and the ground has a low impact, i.e., even a large increase of the distance from 10 to 500 m reduces the capacitance by less than 50% according to FEM simulations.

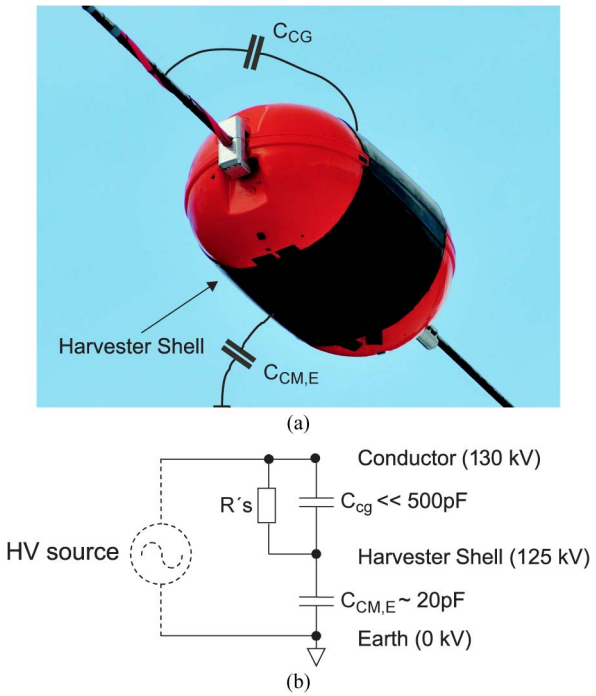

Fig. 5. To obtain the required power from the energy harvester, the maximum divider ratio of the two capacitances (C_{CG} between conductor line and harvester shell, including all parasitic paths, and $C_{CM,E}$ between harvester shell and earth) must be less than 25:1 to yield sufficient power through the equivalent load impedance $R's$ which equals the power-harvesting circuitry. The depicted voltage levels and capacitances are resulting from the power estimation (compare Section II-C). (a) Harvester prototype on a 220-kV overhead power line. (b) Equivalent circuit of the conductor–harvester–earth system.

Details on the circuitry to make this displacement current appropriate for powering a measurement circuitry are given in Section II-C.

Fig. 5(a) and (b) shows a photograph and the equivalent circuit of the conductor–harvester–earth system, respectively. The black portion in the photograph is coated with aluminium foil on the inner side, representing the cylinder capacitor.

C. Data Transmission, Power Estimation, and Circuitry Design

For an autonomous measurement system on a high-voltage overhead power line, the most promising way of transferring measurement data to a host is a wireless connection via a commercial GSM network. Using this well-established technology allows for the independent operation of a single device. In addition, this module may act as a GSM access point for a wireless sensor network of multiple devices along a power line. This network would then be capable of monitoring a complete line system (compare [16] and [17]).

In the current setup, the measurement chain comprises an integrated measurement circuitry, a microcontroller, and a GSM modem [19], which is designed for operation from a single lithium battery cell at 3.7–4.2 V. The GSM modem is the major energy consumer of the complete measurement chain, as the microcontroller's current consumption is typically below

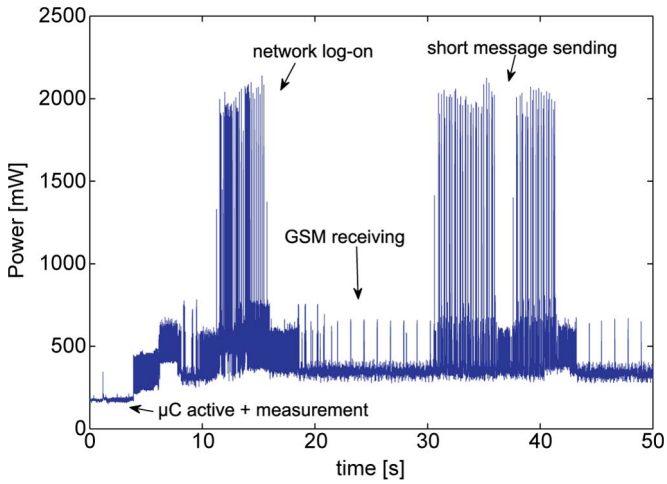

Fig. 6. Power consumption for one complete measurement and data transmission cycle. In the first few seconds, only the microcontroller and the measurement circuitry are active, requiring very low power. Then, the GSM modem is turned on. After powering up, the GSM modem is in receive mode (checking the network availability), consuming approximately 600 mW. Then, the GSM modem switches to transmission mode for the network log-on process. The power demand rises drastically to more than 2 W (12–16 s). Then, the modem switches to idle mode, still remaining connected to the network. The modem is configured by the microcontroller to send a short message and receives the text to be transmitted. The wireless data transfer starting at 30 s causes a high (but pulsed) power demand. At the end of the measurement and transmission sequence, the GSM modem remains idle.

20 mA and the measurement circuitry only consumes several milliwatts. The peak power of the GSM modem amounts up to 8 W (current peaks demanded by the transmitter can be up to 2 A). The power supply circuitry of the energy harvester has been developed to fulfill these requirements, and additionally, capacitors and a backup lithium-ion rechargeable battery have been added to stabilize the supply voltage. In Fig. 6, a complete measurement and data transmission cycle was recorded. It is shown that the microcontroller requires approximately 100 mW, while the GSM modem consumes up to 2000 mW for short periods of time (these values are already smoothened by capacitors; in fact, the peak consumption is four times as high as that for time periods of approximately 5 ms). The total average of the depicted cycle is below 350 mW and can be further reduced. This power demand is the major design parameter for the harvesting circuitry.

Assuming a displacement current of 100 μA, a voltage of 5000 V between the conductor and the harvester shell is required to achieve an output power of 500 mW, which is sufficient for the continuous operation of the measurement system.

D. Problem Description: Parasitic Paths and Limitations

As the energy harvester principle is based on a capacitive voltage division, the parasitic path between the conductor line and the harvester common mode ground (CMG) potential must be avoided to keep the device operational (compare Fig. 7). Assuming a capacitance $C_{CM,E}$ of 20 pF between the harvester shell and the ground (at a 10-m height), a harvester clamping voltage of 5 kV, and a system voltage of 220 kV line to line

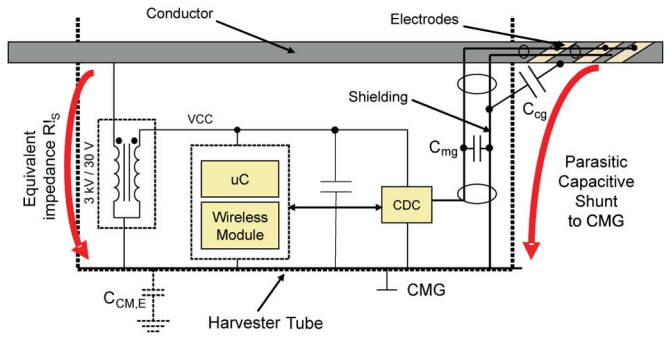

Fig. 7. Parasitic link due to the supply lines of the sensor circuitry (CDC) leads to a capacitive shunt between the conductor and the CMG: The connection between the CDC and the sensor electrodes on the conductor line surface is established by means of a coaxial cable with a capacitance C_{mg} of approximately 100 pF/m. At least two measurement cables are necessary to form a measurement capacitance. The length of the measurement cables has to be chosen in order to provide sufficient distance between the sensitive electrode areas and the harvester shell (approximately 1 m in the current design). The parasitic capacitance C_{CG} formed by the shielding of the coaxial cable and the conductor line provides the main contribution (several hundreds of picofarads) to the parasitic capacitive shunt between the conductor line and the CMG.

(i.e., an approximately 130-kV rms voltage), the capacitance C_{CG} between the conductor and the harvester shell (including all parasitic paths) must not exceed 500 pF. The parasitic capacitance between the shielding of the coaxial cables toward the sensor wires (estimated over 100 pF/m—approximately 5 m of the total cable length is used in the current setup) and the conductor line already by far exceeds this value. In this case, the displacement current to the environment would no longer pass through the transformer (i.e., the equivalent load impedance $R's$) but through the parasitic path formed by C_{CG} and would be lost for harvesting.

Operating integrated measurement circuitry in the environment of a high-voltage overhead power transmission line poses further problems, among which is the high magnetic field strength in the vicinity of the conductor. The electrical field gradient is highest in the immediate vicinity of the conductor too, but it is easier to shield. However, the sensor has to be exposed to this environment to take icing measurements on the conductor. The conductor itself can carry peak currents of several thousands of amperes. To avoid problems due to the strong magnetic field in this area, it was decided to mount the measurement circuitry on the inner side of the harvester shell in a maximum distance from the conductor. This also ensures a known environment with respect to the electrical field. As the circuitry is mounted on the harvester shell, it is useful to define this potential also as the ground potential (CMG) of the circuitry. CDCs most often refer their signal levels (excitation outputs and receiver inputs) to the electrical ground.

The following conditions have to be considered.

1) The communication circuitry needs to reside as far as possible from the conductor to keep the induced voltages in the antenna as low as possible.
2) The CDCs should reside as close as possible to the conductor to minimize the 50-Hz disturbances between the measurement ground and the CDC receiver inputs.

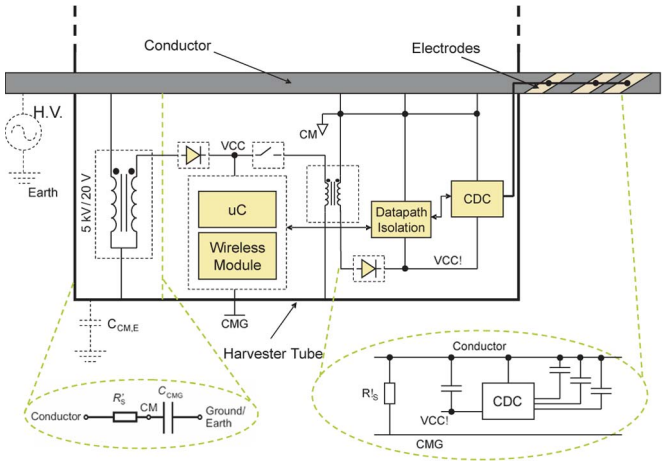

Fig. 8. Schematic of the measurement chain with decoupled measurement circuitry.

3) The total parasitic impedance of the circuitry between the conductor and the harvester shell has to remain below a certain limit because the capacitance between the conductor and the harvester shell (i.e., the divider ratio) is crucial for the operation of the energy harvester.
4) The sensor cables need to be shielded to be sensitive only in the desired area. A shield potential needs to be defined. If the shield potential is set to ground potential (i.e., the harvester shell, CMG), the parasitic capacitances would by far exceed the limits that need to be respected for the operation of the energy harvester.

Given this, the following design rules should be obeyed.

1) The measurement circuitry needs to be decoupled from the harvesting and communication circuitry. Consequently, there are two ground levels (harvester ground and measurement ground) with a potential difference of 5000 V.
2) Isolated data transmission is required between the communication circuitry and the measurement circuitry.
3) Isolated power transmission is required to power the measurement circuitry.
4) All capacitances introduced by these data and power paths are parasitic capacitances with respect to the harvester shell and should be kept as low as possible.

III. Proposed Solution

For the mentioned reasons, the decoupling of the sensor front end from the microcontroller printed circuit board (PCB) is required. Consequently, the entire sensor circuitry (i.e., the sensor electrodes and the measurement circuitry) has to be electrically separated from the microcontroller and the communication circuitry. This approach also allows the usage of the conductor line as the measurement ground potential (denoted as CM in Fig. 8). For the field-test prototype, the decoupling was realized by two means.

1) Bidirectional I^2C bus buffers [21] and optical couplers [22] suited for an isolation voltage of 50 kV. Laboratory tests have also been successful using readily available components for an 800-V isolation voltage. However, these parts are certified to withstand a voltage of 5 kV for 1 min only and are thus not suitable for an application in the field.
2) A power transformer. The sensor circuitry has to be supplied with the required power (several milliwatts). This is established by a small isolated transformer operating at a high switching frequency.

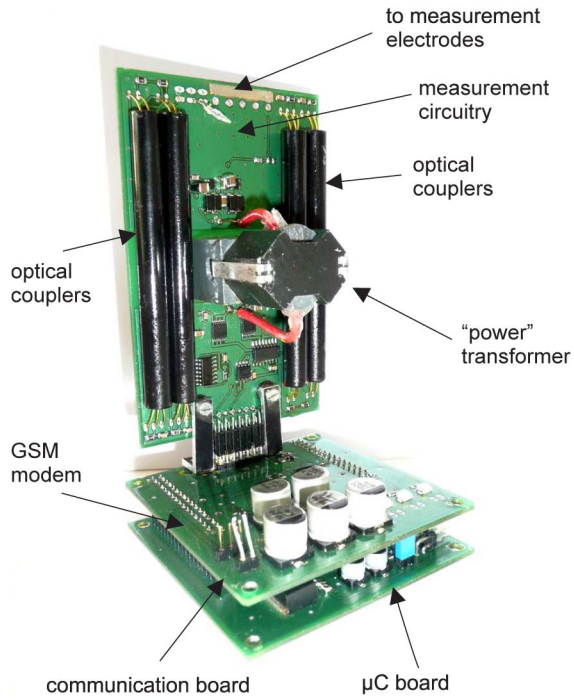

Fig. 9. Photograph of the complete measurement PCB stack as used for the laboratory tests. In order to keep the influence on the electric field distribution within the harvester shell as low as possible while minimizing disturbances in the circuitry, the sensor board has been mounted in a 90° angle with respect to the microcontroller and communication circuitry.

Fig. 8 shows a sketch of the proposed approach. The primary winding of the 5-kV/20-V transformer is connected to both the conductor line and the energy harvester's outer shell. The transformer output is regulated to the required supply voltage (VCC) of 4 V with respect to the harvester shell (CMG). The optical couplers feature high-voltage isolation for the data path between the microcontroller board and the sensor circuitry. The small transformer establishes the transfer of the electrical power (a few milliwatts) required by the sensor circuitry. On the secondary side of this transformer, the potential of the conductor is referred to as ground potential (CM).

Furthermore, the sensor circuitry and the decoupling board are mounted in vertical orientation with respect to the microcontroller and communication board to keep further parasitic capacitances low and to lower the effect of the magnetic field strength on the measurement circuitry (compare Fig. 9).

Fig. 10 shows a block diagram of the decoupled circuitry.

IV. Experimental Setup and Results

A. Preliminary Tests

The modified measurement circuitry has been preliminarily tested under laboratory conditions using a 6-kV stray

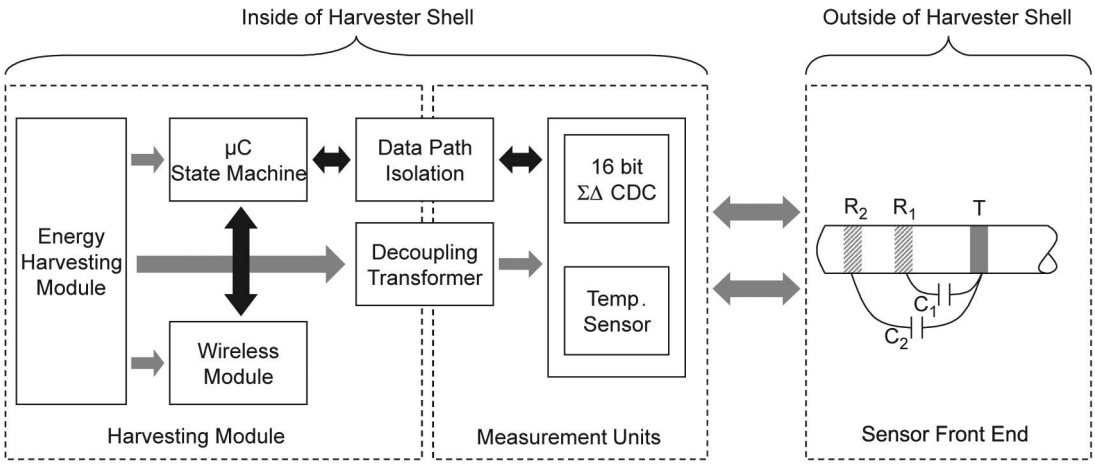

Fig. 10. Overview of the complete decoupled measurement setup. The energy harvester circuitry supplies the necessary power to the microcontroller and communication board. Power supply is provided to the decoupled secondary side of the system via the decoupling transformer. The data path to the decoupled secondary side is established by means of bidirectional I^2C bus buffers [21] and optical couplers [22] suited for an isolation voltage of 50 kV.

transformer. The isolated CDC unit was connected to an I^2C-to-Universal Serial Bus module. The measurement data were read using a National Instruments LabView environment. A sheet of paper cloth was put onto the conductor line. The dry value was recorded, and after some seconds, water was dropped onto the conductor. Thus, a water layer of certain thickness was kept around the conductor (i.e., it covered the measurement electrodes). The capacitance measurement result (a significant decrease in interelectrode capacitance) met the expectations. However, the purpose of this test was the evaluation of the impact of the 50-Hz alternating field on the measurement, particularly with respect to the signal-to-noise ratio. It was shown that the used filters are sufficient to suppress the impact (compare Section IV-C for measurement results obtained during a field test). In addition to that, the filtering of the transmitted and received signals can be implemented by discrete filter structures at the excitation and the receiver channels of the CDC. This will be necessary to damp the spikes originating from power switching processes and to further improve electromagnetic compatibility robustness.

B. High-Voltage Laboratory Tests

The measurement chain was tested in the Graz University of Technology high-voltage laboratory. Conductor icing cannot be simulated in this environment, but since it is comparatively easy to distinguish an ice layer from a dry conductor or a wet conductor (measurement signals for dry and wet conductors have been recorded during the laboratory high-voltage test of the measurement circuitry), a sample of a conductor line with a prefabricated ice shell was used to observe the ice melting process (with an ice layer thickness of approximately 50 mm). The details of the measurement setup are shown in Fig. 11. Coaxial cables made from PTFE (Teflon) were used for the sensor leads. The material can withstand the desired temperature range and is corona proof. It has to be noted that the measured ice quality in this experiment differs from real-world ice qualities due to its different origin. In most occurrences of natural icing, the overall air content of the accreted ice will be higher, thus delivering a smaller measurement signal.

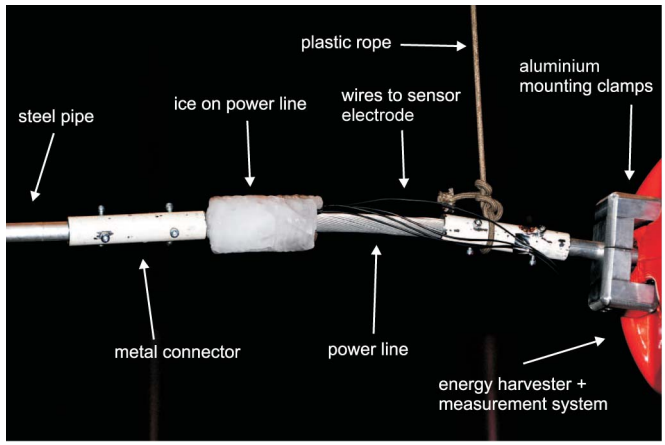

Fig. 11. Measurement electrodes and ice block frozen onto a conductor line sample during the measurement on the high-voltage conductor in the high-voltage laboratory.

The system started its operation at 90 kV, equivalent to a transmission system voltage of 153 kV line to line.

C. Field Tests

In February 2010, the prototype was mounted on a 220-kV line on an Austrian mountain pass at approximately 1000 m above sea level. Several icing events have been detected, one of which is discussed in this section. Fig. 12 depicts the measurement data for an example icing event with a duration of 35 h (compare [23]). The capacitance readouts C_1 and C_2 denote the coupling capacitances between the common transmitter electrode T and the receiver electrodes R_1 and R_2, respectively (compare Fig. 10). The nominal capacitance values obtained for a dry conductor amount to 275 fF for the capacitance C_1 (near electrode) and 26 fF for the capacitance C_2 (far electrode). After approximately 21 h, the measured conductor temperature increases, and the ice layer is melting. The standard deviation of the measurement (one transmitted

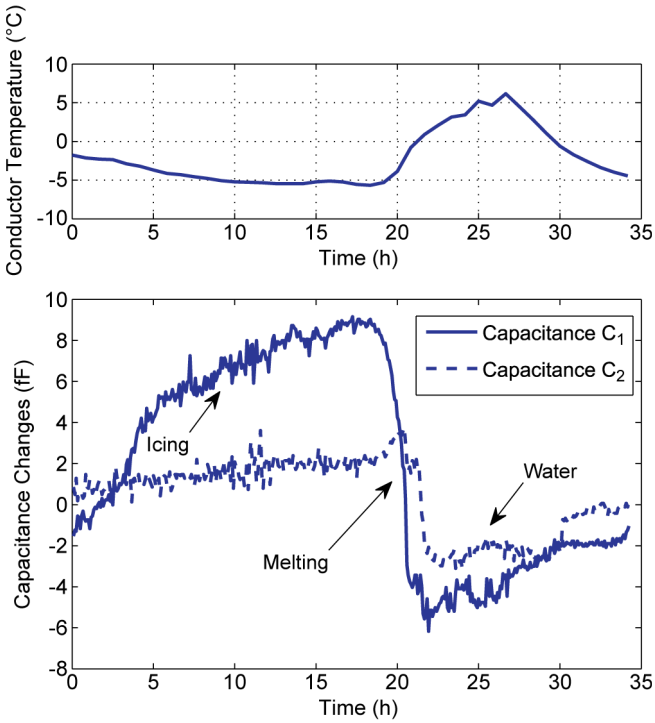

Fig. 12. Measurement data from an example icing measurement (compare [23]). (Top) During the observation period, the temperature of the conductor varied from approximately -5 °C to 5 °C. Please note that the measured conductor temperature is delayed due to the thermal capacity of the clamps. (Bottom) Change of measurement capacitances C_1 and C_2. In the first section, an ice layer is forming up. Consequently, the capacitances increase with respect to the nominal capacitances obtained at dry conditions. Later, all the measurement capacitances are lower than their nominal ("dry") values. This indicates a wet conductor (i.e., melting of the ice layer).

measurement value represents the average over 80 samples acquired with a high sampling rate) is constantly around 0.13 fF, while during the melting process, it rises up to 0.95 fF, which is within the expected range due to the fast signal change.

V. Conclusion and Outlook

In this paper, the design of a prototype for icing detection on high-voltage overhead power lines has been reported. The measurement system obtains the power necessary for operation from the electrical field of a high-voltage overhead power line. Measurement data are transmitted to a remote computer via a GSM network. The main measurands are capacitances in the picofarad range and capacitance changes in the femtofarad range due to the presence of water or ice on the conductor. By decoupling the harvester and communication circuitry from the measurement circuitry and thus introducing separated reference potentials, optimal mounting positions of all parts of the circuitry can be chosen.

In February 2010, the prototype was prepared for a field test and mounted on a 220-kV line on an Austrian mountain pass at approximately 1000 m above sea level. The field prototype successfully acquired and transmitted measurement data via a GSM network link. The next steps comprise investigations in the field, as the icing process and the ice qualities will be different from those observed in laboratory experiments. As certain icing conditions occur rarely, this will involve enduring investigations at different locations.

References

[1] S. Valsan and K. Swarup, "High-speed fault classification in power lines: Theory and FPGA-based implementation," *IEEE Trans. Ind. Electron.*, vol. 56, no. 5, pp. 1793–1800, May 2009.

[2] M. Di Santo, A. Vaccaro, D. Villacci, and E. Zimeo, "A distributed architecture for online power systems security analysis," *IEEE Trans. Ind. Electron.*, vol. 51, no. 6, pp. 1238–1248, Dec. 2004.

[3] "Assessment study on sensors and automation in the industries of the future," U.S. Dept. Energy, Washington, DC, 2004.

[4] M. Lacroix, L. Brouillette, and A. Blais, "Hydro Quebec's de-icing system: Automated overhead line monitoring and de-icing system," in *Proc. Cigre Session, B2-211*, Paris, France, 2008, pp. 1–7.

[5] M. Moser, H. Zangl, T. Bretterklieber, and G. Brasseur, "An autonomous sensor system for monitoring of high voltage overhead power supply lines," *Elektrotech. Informationstechnik*, vol. 126, no. 5, pp. 214–219, May 2009.

[6] K. Savadjiev and M. Farazaneh, "Modeling of icing and ice shedding on overhead power lines based on statistical analysis of meteorological data," *IEEE Trans. Power Del.*, vol. 19, no. 2, pp. 715–721, Apr. 2004.

[7] M. Muhr, S. Pack, S. Jaufer, W. Haimbl, and A. Messner, "Development and implementation of a monitoring-system to increase the capacity of overhead lines," in *Proc. Cigre Session, B2-101*, Paris, France, 2008, pp. 1–6.

[8] H.-J. Draeger, D. Hussels, and R. Puffer, "Experiences with the weather parameter method for the use in overhead line monitoring systems," in *Proc. Cigre Session, B2-107*, Paris, France, 2008, pp. 1–8.

[9] M. Moser, H. Zangl, and G. Brasseur, "Icing detector for overhead power transmission lines," in *Proc. IEEE Instrum. Meas. Technol. Conf.*, Singapore, 2009, pp. 1105–1109.

[10] L. K. Baxter, *Capacitive Sensors, Design and Applications*. Piscataway, NJ: IEEE Press, 1997.

[11] B. George, H. Zangl, T. Bretterklieber, and G. Brasseur, "Seat occupancy detection system based on capacitive sensing," *IEEE Trans. Instrum. Meas.*, vol. 58, no. 5, pp. 1487–1494, May 2009.

[12] H. Zangl, T. Bretterklieber, and G. Brasseur, "Energy harvesting for on-line condition monitoring of high voltage overhead power lines," in *Proc. IEEE Instrum. Meas. Technol. Conf.*, Victoria, BC, Canada, 2008, pp. 1364–1369.

[13] N. D. Sadanandan and A. H. Eltom, "Power donut system laboratory test and data analysis," in *Proc. IEEE Souteastcon*, New Orleans, LA, April 1–4, 1990, pp. 675–679.

[14] L. Du, C. Wang, X. Li, L. Yang, Y. Mi, and C. Sun, "A novel power supply of online monitoring systems for power transmission lines," *IEEE Trans. Ind. Electron.*, vol. 57, no. 8, pp. 2889–2895, Aug. 2010.

[15] D. Dondi, A. Bertacchini, D. Brunelli, L. Larcher, and L. Benini, "Modeling and optimization of a solar energy harvester system for self-powered wireless sensor networks," *IEEE Trans. Ind. Electron.*, vol. 55, no. 7, pp. 2759–2766, Jul. 2008.

[16] V. Gungor and G. Hancke, "Industrial wireless sensor networks: Challenges, design principles, and technical approaches," *IEEE Trans. Ind. Electron.*, vol. 56, no. 10, pp. 4258–4265, Oct. 2009.

[17] V. C. Gungor, B. Lu, and G. P. Hancke, "Opportunities and challenges of wireless sensor networks in smart grid," *IEEE Trans. Ind. Electron.*, vol. 57, no. 10, pp. 3557–3564, Oct. 2010.

[18] T. Bretterklieber, H. Zangl, M. Motz, T. Werth, and D. Hammerschmidt, "Versatile sensor front end for low-depth modulation capacitive sensors," in *Proc. IEEE Instrum. Meas. Technol. Conf.*, Victoria, BC, Canada, May 2008, pp. 830–835.

[19] Telit Communications S.p.A., GM862 Modem QUAD GPS Data Sheet, 2009.

[20] Analog Devices Inc., ADUM2251: Hot-Swappable Dual I2C Isolators, 5 kV, 2007.

[21] NXP Semiconductors, P82B96: Dual Bi-Directional Bus Buffer, 2004.

[22] Optek Technology, OPI155 High-Speed Optically Coupled Isolator, 2007.

[23] M. J. Moser, T. Bretterklieber, H. Zangl, and G. Brasseur, "Capacitive icing measurement in a 220 kV overhead power line environment," in *Proc. IEEE Int. Conf. Sens.*, Waikoloa, HI, 2010, pp. 1754–1757.

Michael J. Moser (S'08) was born in Eisenerz, Austria, in 1981. He received the Dipl.-Ing. degree in electrical engineering and sound engineering from Graz University of Technology, Graz, Austria, and the University of Music and Performing Arts, Graz, in 2007. He is currently working toward the Ph.D. degree in the Sensors and Instrumentation Research Group, Institute of Electrical Measurement and Measurement Signal Processing, Graz University of Technology.

He is currently a Research Assistant with the Sensors and Instrumentation Research Group. His research interests include capacitive sensors, with emphasis on the wireless and smart capacitive sensors, capacitive flow measurement, and capacitive icing detection.

Thomas Bretterklieber (M'08) was born in Graz, Austria, in 1978. He received the Dipl.-Ing. degree in telematics and the Dr. Techn. degree in electrical engineering from the Graz University of Technology (TU Graz), Graz, in 2001 and 2008, respectively.

He is currently a Senior Researcher with the Sensors and Instrumentation Group, Institute of Electrical Measurement and Measurement Signal Processing, TU Graz. His research interests focus on the design and optimization of robust and reliable sensors for automotive and industrial applications and mixed-signal integrated circuit design.

Hubert Zangl (M'05) received the Dipl.Ing. degree in telematics, the Dr. Techn. degree in electrical engineering, and the venia docendi for sensors and instrumentation from the Graz University of Technology (TU Graz), Graz, Austria, in 2001, 2005, and 2009, respectively.

Since 2010, he has been an Associate Professor at the Institute of Electrical Measurement and Measurement Signal Processing, TU Graz, in the Sensors and Instrumentation Group. He has authored or coauthored more than 100 international scientific publications. He is the holder of several patents. His research interests focus on sensor design and optimization, sensor signal processing, and passive/semiactive wireless sensor interfaces.

Georg Brasseur (M'94–SM'97–F'10) was born in Vienna, Austria, in 1953. He received the Dipl.-Ing. degree in electrical engineering in 1979, the Ph.D. degree in technical science in 1985, and the venia docendi in industrial electronics from the Vienna University of Technology, Vienna.

Since 1999, he has been a Full Professor with the Institute of Electrical Measurement and Measurement Signal Processing, Graz University of Technology (TU Graz), Graz, Austria. From 2001 to 2008, he was the Chair of the Christian Doppler Laboratory for Automotive Measurement Research, and in 2004 and 2005, he was the Dean of the Faculty of Electrical and Information Engineering, TU Graz. He has authored or coauthored over 100 technical papers. He is the holder of several patents. His research interests focus on automotive sensors, capacitive-sensing devices, analog circuit design, automotive electronics, and actuators.

Dr. Brasseur is a Cochair of the IEEE Instrumentation and Measurement Technical Committee TC20 and is a member of the Austrian Academy of Sciences and the Austrian and German Association of Professional Electrical Engineers.